

Re-examining extreme carbon isotope fractionation in the coccolithophore *Ochrosphaera neapolitana*

Received: 5 January 2022

Hongrui Zhang ^{1,2}✉, Ismael Torres-Romero ^{1,2}✉ & Heather M. Stoll ¹

Accepted: 18 November 2022

Published online: 12 December 2022

Check for updates

ARISING FROM Y.-W. Liu et al. *Nature Communications* <https://doi.org/10.1038/s41467-018-04463-7> (2018)

In coccolithophores, stable isotopes recorded in both the calcite exoskeleton (coccoliths), and organic carbon (C_{org}), can reflect their physiological response to environment, and thereby have a wide usage in paleoclimate and biogeochemistry studies. Recently, Liu et al.¹ reported that coccolithophore *Ochrosphaera neapolitana* has much more positive carbon isotope fractionations relative to dissolved inorganic carbon (DIC) in both coccolith and C_{org} compared with those published previously for other species^{2–4} and attributed such unexpected positive carbon isotope fractionations to a unique carbon pathway in this species. However, we find that these extreme isotopic fractionations should be attributed to the poor constraints in DIC carbon isotope ratios instead of the coccolithophores' physiological response to $p\text{CO}_2$. More careful measurements of DIC carbon isotope would benefit data interpretations and comparisons in future laboratory culture works focusing on phytoplankton's response to ocean acidification.

In order to study this unusual isotopic fractionation, we carried out another independent culture of *O. neapolitana* under a low CO_2 environment ($p\text{CO}_2 \approx 254\text{ppm}$ and $\text{CO}_2(\text{aq}) \approx 8.7\ \mu\text{M}$). The results of carbon isotope fractionation show no exaggerated positive values in neither coccolith nor C_{org} (Fig. 1). The carbon isotope fractionation between coccolith and DIC ($\Delta^{13}\text{C}_{\text{coccolith-DIC}} = \delta^{13}\text{C}_{\text{coccolith}} - \delta^{13}\text{C}_{\text{DIC}}$) is $-1.86 \pm 0.43\text{‰}$ (standard deviation of three biological replicates) and that of C_{org} ($\Delta^{13}\text{C}_{\text{Corg-DIC}} = \delta^{13}\text{C}_{\text{Corg}} - \delta^{13}\text{C}_{\text{DIC}}$) is $-23.14 \pm 0.57\text{‰}$, which are in the same range as published carbon isotope fractionations of other species.

We propose that the extreme positive carbon isotope fractionations and fractionation trend with $p\text{CO}_2$, originally reported by Liu et al.¹ might be caused by inaccurate estimation of the DIC carbon isotope ratio ($\delta^{13}\text{C}_{\text{DIC}}$). Instead of directly measuring $\delta^{13}\text{C}_{\text{DIC}}$ during culture, the authors assumed that $\delta^{13}\text{C}_{\text{DIC}}$ reached equilibrium with CO_2 sources through the whole experiment. However, in reality, the $\delta^{13}\text{C}_{\text{DIC}}$ could be positively shifted by two processes, (1) the isotopic disequilibrium between $\text{CO}_2(\text{g})$ and DIC during bubbling and (2) the selective uptake of light carbon by algae photosynthesis during culture.

As previously suggested, seawater culture medium should be bubbled at least overnight to achieve a stable carbonate system⁵. Yet, the isotopic equilibrium is much slower than the chemical equilibrium⁶, because the carbon atoms need to be fully exchanged between gas phase and liquid phase before reaching an isotopic equilibrium. Moreover, all culture experiments in Liu et al.¹ were carried out using 38 L glass aquaria, thus increasing the time for such a large DIC pool to reach isotopic equilibrium with the gas phase. In Liu et al.¹, the details in aeration process, such as aeration time and initial $\delta^{13}\text{C}_{\text{DIC}}$, were not described. Based on the final $p\text{CO}_2$ in all treatments being lower than the target $p\text{CO}_2$ by at least 20%, we infer that the seawater media were pre-bubbled before the incubation of coccolithophores and that there was no further CO_2 aeration during the culture. To evaluate the extent of isotopic disequilibrium in the pre-bubbling process, here we carry out isotopic simulations to trace the carbon atom exchanging process between DIC and CO_2 source (more details in Methods and Supplementary Note 1).

One key parameter in the simulations is the carbon atom exchanging rate constant between $\text{CO}_2(\text{g})$ and $\text{CO}_2(\text{aq})$ (k_E). In our previous work, we measured this constant in two photobioreactor systems featuring aeration with specified CO_2 concentration; this constant ranged from 3.4×10^{-5} to $8.7 \times 10^{-5}\ \text{mol s}^{-1}\ \text{atm}^{-1}$. We conduct simulations using k_E ranging from 10^{-4} to $10^{-3}\ \text{mol s}^{-1}\ \text{atm}^{-1}$. For reproducing the DIC carbon isotope evolution in Liu et al.¹, a k_E of $\sim 3.6 \times 10^{-4}$ is more realistic considering their gas flux was $1.5\ \text{L min}^{-1}$, 6 times as our bubbling system in ETH Zurich. Another important parameter is the initial carbon isotope ratio difference between DIC and CO_2 source. Based on equilibrium $\delta^{13}\text{C}_{\text{DIC}}$ described by Liu et al.¹, we back-calculated the isotopic signatures of the CO_2 sources employed among treatments in Liu et al.¹. These range from -14‰ to -38‰ (Supplementary Table S1). A larger initial difference can potentially cause a more significant disequilibrium between DIC and $\text{CO}_2(\text{g})$ leading to an underestimation of $\delta^{13}\text{C}_{\text{DIC}}$ (as simulated in Fig. 2) and thereby more positive coccolith and C_{org} carbon isotope fractionations. For example, the carbon isotope disequilibrium in '280 ppm' treatment could be larger than the disequilibrium in other

¹Geological Institute, ETH Zürich, 8092 Zürich, Switzerland. ²These authors contributed equally: Hongrui Zhang, Ismael Torres-Romero.

✉ e-mail: zhz@ethz.ch; iromero@ethz.ch

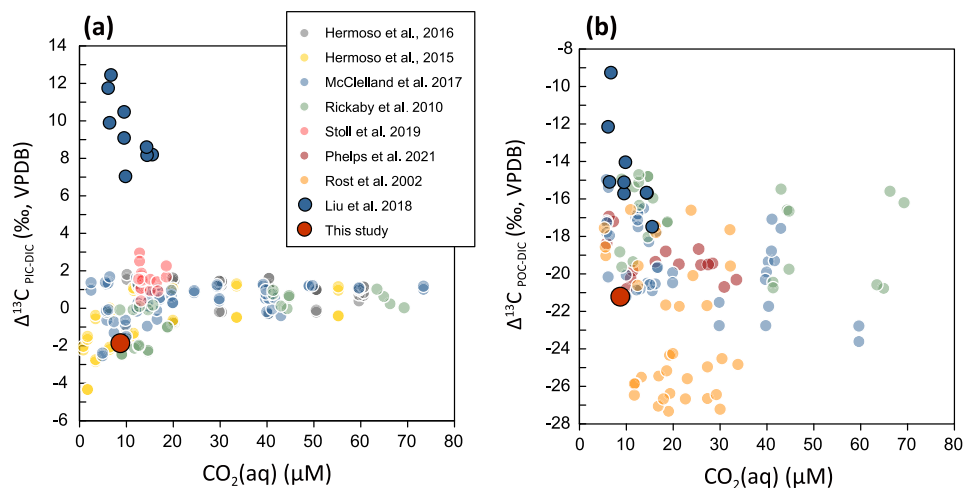


Fig. 1 | Carbon isotope fractionations ($\Delta^{13}\text{C}$) of coccolithophores in different laboratory culture studies. **a Carbon isotope fractionation between PIC (particulate inorganic carbon from harvested cells) and DIC (dissolved inorganic carbon from seawater). **b** Carbon isotope fractionation between POC (particulate organic carbon from harvested cells) and DIC. Markers plotted in red and blue are**

Ochrosphaera neapolitana in this study and in Liu et al.¹, respectively. Markers in other colors are results from other publications^{2-4,12-15} using different species of coccolithophores including *Coccolithus pelagicus*, *Gephyrocapsa oceanica*, *Calcidiscus leptoporus*, and *Emiliania huxleyi*.

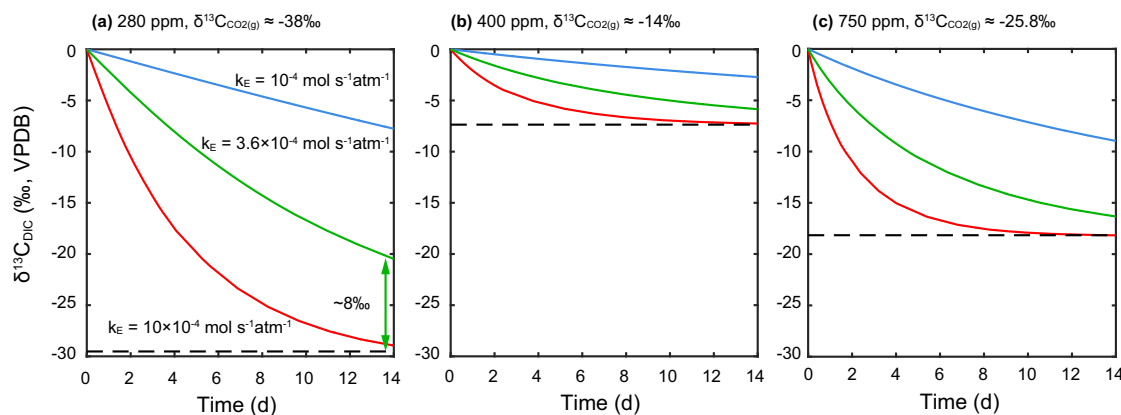


Fig. 2 | Simulated DIC carbon isotope ratios evolution during bubbling. Panel a, b, c are simulations for different $p\text{CO}_2$ and initial $\delta^{13}\text{C}_{\text{DIC}}$. Blue curves: $k_E = 10^{-4} \text{ mol s}^{-1} \text{ atm}^{-1}$ (a slower equilibrium). Red curves: $k_E = 10^{-3} \text{ mol s}^{-1} \text{ atm}^{-1}$ (a faster equilibrium). Green curves: $k_E = 3.6 \times 10^{-4} \text{ mol s}^{-1} \text{ atm}^{-1}$

(potential exchanging rate for Liu et al.¹). The black dashed lines represent the isotopic equilibrium $\delta^{13}\text{C}_{\text{DIC}}$. The disequilibrium between DIC and gas in 280 ppm treatment after two weeks of bubbling is marked by the vertical green arrows.

two treatments by up to 8‰ even after two weeks aeration (green line in Fig. 2a). Hence, we infer that the isotopic disequilibrium between gas phase and liquid phase during the pre-bubbling process is the main reason why the calculated carbon isotope fractionations in ‘280 ppm’ treatment were much more positive than the results in the other two treatments, instead of the lower $p\text{CO}_2$.

Photosynthesis preferentially takes up the light carbon leading to a positive shift of remaining DIC. Ignoring the carbon isotope effect of calcification (much smaller effect compared with photosynthesis), this positive shift in DIC carbon isotope ratio can be estimated by mass balance (Supplementary Note 3). Given a cell density of $10^5 \text{ cell mL}^{-1}$ as in Liu et al.¹, the carbon isotope fractionation could be as large as +3‰. We suggest that this DIC carbon isotope shift during culture can explain -20% of the abnormal carbon isotope fractionation in Liu et al.¹, especially the large carbon isotope differences among replicates within the same treatment.

Our culture data and simulations show evidence that the carbon isotope fractionation results in Liu et al.¹ could have a significant bias due to the lack of direct $\delta^{13}\text{C}_{\text{DIC}}$ measurements. Despite acknowledging their values might have an offset (the absolute values on fractionation

could differ from real values), they still claimed that the trend of carbon isotope fractionation on $p\text{CO}_2$ should be robust. Nevertheless, such trend in Fig. 3 of Liu et al.¹ would already not be significant when we account for the different disequilibrium offsets among the three treatments. Indeed, simulations of $\delta^{13}\text{C}_{\text{DIC}}$ evolution suggest that the offset in ‘280 ppm’ treatment could be as large as 10‰ more positive than the other two treatments. Thus, their measurements do not support their conclusion that the calcification and photosynthesis of *O. neapolitana* share the same carbon pool.

Carbon isotope techniques in laboratory cultures have been widely used to trace the ocean acidification effects on phytoplankton, and thereby calibrate a robust $p\text{CO}_2$ proxy in the paleo-climate field. Considering the importance of culture studies with isotopic measurement, cautions should be exercised in experiment design. First, a larger volume of culture medium entails a longer isotopic equilibrium time during the CO_2 aeration process, which should be noted for future work especially using bubbling methods. More importantly, the $\delta^{13}\text{C}_{\text{DIC}}$ should be measured directly to assess fractionation correctly in future isotopic studies. Only measuring the DIC carbon isotope at the beginning of culture is not enough for the batch cultures, because the

positive shifts of DIC carbon isotope due to photosynthesis could be as large as 3‰. By following the recommendations described here, we can make the isotopic results comparable and help to better understand the phytoplankton's response to ocean acidification.

Methods

Laboratory culture

Ochrosphaera neapolitana (RCC1357) was precultured in K/2 medium without Tris buffer⁸ using artificial seawater (ASW) supplemented with NaHCO₃ and HCl to yield an initial DIC of 2050 μM. In triplicate, 1-L bottles were filled with 150 mL of seawater medium with air in the bottle headspace and inoculated with a mid-log phase preculture at an initial cell concentration of 10⁴ cells mL⁻¹. Cultures were grown at 18 °C under a warm white LED light at 100 ± 20 μE on a 16h-light/8h-dark cycle. Bottles were orbitally shaken at 60 rpm to keep cells in suspension. Cell growth was monitored with a MultiSizer 4e particle counter and sizer (Beckman Coulter). At 1.4 × 10⁵ cells mL⁻¹, cells were diluted up to 300 mL to 2–3 × 10⁴ cells mL⁻¹ and harvested after 2 days of more exponential growth up to 7.9 ± 0.6 × 10⁴ cells mL⁻¹. More detailed culture results are listed in the Supplementary Note 1.

Immediately after harvesting, pH was measured using a pH probe calibrated with Mettler Toledo NBS standards (it should be noted here that high ionic strength calibration standards would be optimal for pH measurement of liquids like seawater). There was a carbonate system shift during the batch culture and more details are shown in Supplementary Fig. S1. Cells in 50 mL were pelleted by centrifuging at -1650 × g for 5 min. Seawater supernatant was analyzed for DIC and δ¹³C_{DIC} by injecting 3.5 mL into an Apollo analyzer and injecting 1 mL into He-flushed glass vials containing H₃PO₄ for the Gas Bench.

For seawater DIC, an Apollo SciTech DIC-C13 Analyzer coupled to a Picarro CO₂ analyzer was calibrated with in-house NaHCO₃ standards dissolved in deionized water at different known concentrations and δ¹³C values from -4.66 to -7.94‰. δ¹³C_{DIC} in media were measured with a Gas Bench II with an autosampler (CTC Analytics AG, Switzerland) coupled to ConFlow IV Interface and a Delta V Plus mass spectrometer (Thermo Fischer Scientific). Pelleted cells were snap-frozen with N₂ (l) and stored at -80 °C. For PIC analysis, pellet was resuspended in 1 mL methanol and vortexed. After centrifugation, the methanol phase with extracted organics was removed and the pellet containing the coccoliths was dried at 60 °C overnight. About 300 mg of dried coccolith powder were placed in air-tight glass vials, flushed with He and reacted with five drops of phosphoric acid at 70 °C. PIC δ¹³C and δ¹⁸O were measured by the same Gas Bench system. The system and above-mentioned in-house standards were calibrated using international standards NBS 18 (δ¹³C = -5.01‰, δ¹⁸O = +23.00‰) and NBS 19 (δ¹³C = +1.95‰, δ¹⁸O = +2.2‰). The analytical error for DIC concentration and δ¹³C is <10 μM and 0.1‰, respectively.

POC and PON were determined from cells harvested on pre-combusted QFF filters and deep-frozen until analysis. Inorganic carbon from cells on filters was removed by fuming sulfuric acid during 24 h. Filters were placed inside a desiccator on a porous tray and 50 mL sulfuric acid below was fumed with a vacuum pump. Gases were evacuated and filters were further dried at 60 °C overnight. Right before Elemental Analysis (EA), filters were compacted and wrapped into tin cups with the help of tweezers and a press. Samples loaded on a 96-well plate were combusted in the oxidation column at 1020 °C of a Thermo Fisher Flash-EA 1112 coupled with a ConFlow IV interface to a Thermo Fisher Delta V-IRMS (isotope ratio mass spectrometer). Combustion gas passed through a reduction column at 650 °C producing N₂ and CO₂ which were separated by chromatography and into a split to the IRMS for an on-line isotope measurement.

Simulations of carbon isotope evolution during aeration

The DIC carbon isotope evolution model is simplified from the model in Zhang et al.⁷ The exchanging rate (with a unit of mol s⁻¹) between CO₂(g) and CO₂(aq) depends on the CO₂ gradient and exchanging rate constant (k_E, with a unit of ppm s⁻¹): ER = k_E(CO_{2(g)} - k_HCO_{2(aq)}), where the k_H is Henry's law constant with a unit of ppm μM⁻¹. The evolutions of DIC and DIC carbon isotope ratios during CO₂ aeration can be calculated by four differential equations:

$$\frac{dC}{dt} = \frac{k_E}{V} (G - C k_H) + (k_{-1}H^+ + k_{-4})C - (k_{+1} + k_{+4}OH^-)B \quad \text{XB1} \quad (1)$$

$$\frac{d^{13}C}{dt} = \frac{k_E}{V} (^{13}G \alpha_{g2aq} - ^{13}C k_H \alpha_{aq2g}) + (k_{+1}^{13} + k_{+4}^{13}OH^-)^{13}B X^{13}B1 - (k_{-1}^{13}H^+ + k_{-4}^{13})^{13}C \quad (2)$$

$$\frac{dB}{dt} = - (k_{-1}H^+ + k_{-4})C + (k_{+1} + k_{+4}OH^-)B \quad \text{XB1} \quad (3)$$

$$\frac{d^{13}B}{dt} = - (k_{-1}^{13}H^+ + k_{-4}^{13})^{13}C + (k_{+1}^{13} + k_{+4}^{13}OH^-)^{13}B \quad X^{13}B1 \quad (4)$$

where capital letters G, C, B, H, and OH represent CO₂(g), CO₂(aq), HCO₃⁻ + CO₃²⁻, H⁺, and OH⁻, respectively. The V stands for volume. The α is the isotopic fractionation, e.g. α_{g2aq} represents the carbon isotope fractionation of CO₂ gas diffusion into liquid phase. The XB1 and X¹³B1 are the fraction of HCO₃⁻ in (HCO₃⁻ + CO₃²⁻) and the fraction of H¹³CO₃⁻ in (H¹³CO₃⁻ + ¹³CO₃²⁻). The XB1 can be calculated by XB1 = $\frac{1}{1 + \frac{k_2}{[H^+]}}$ and the

X¹³B1 can be calculated by X¹³B1 = $\frac{1}{1 + \frac{k_2}{[H^+]}\alpha_{CO_3-HCO_3}}$, where the α_{CO₃-HCO₃} is the carbon isotope fractionation between CO₃²⁻ and HCO₃⁻. The k₊₁ is the reaction rate constant of CO₂ hydration, which can be calculated by ln k₊₁ = 1246.98 - $\frac{61900}{T_k}$ - 183 ln T_k¹⁰. The k₋₁, the reaction rate constant of HCO₃⁻ dehydration, can be calculated from k₊₁, k₋₁ = $\frac{k_{+1}}{K_1}$. The k₋₄ and k₊₄ are the reaction rate constants of CO₂ hydroxylation and HCO₃⁻ dihydroxylation. The k₊₄ is calculated by ln k₊₄ = 17.67 - $\frac{2790.47}{T_k}$ and k₋₄ = k₊₄ $\frac{K_w}{K_1}$, where K_w is the stoichiometric ion product of water. The K₁ and K₂ are the first and second dissociation constants of carbonic acid and in this study, we employed equations from¹¹, in which the K₁ and K₂ were calculated for pH in NBS scale. The reaction rate constants for ¹³C (k₋₁¹³, k₊₁¹³, k₋₄¹³ and k₊₄¹³). The initial values for these differential equations are described in the Supplementary Note 2.

Data availability

All culture data generated in this study can be found in the main text and Supplementary Note 1. Source data are provided with this paper.

References

- Liu, Y. W., Eagle, R. A., Aciego, S. M., Gilmore, R. E. & Ries, J. B. A coastal coccolithophore maintains pH homeostasis and switches carbon sources in response to ocean acidification. *Nat. Commun.* **9**, 2857 (2018).
- Hermoso, M., Chan, I. Z. X., McClelland, H. L. O., Heureux, A. M. C. & Rickaby, R. E. M. Vanishing coccolith vital effects with alleviated carbon limitation. *Biogeosciences* **13**, 301–312 (2016).
- Rickaby, R. E. M., Henderiks, J. & Young, J. N. Perturbing phytoplankton: response and isotopic fractionation with changing carbonate chemistry in two coccolithophore species. *Clim* **6**, 771–785 (2010).
- McClelland, H. L., Bruggeman, J., Hermoso, M. & Rickaby, R. E. The origin of carbon isotope vital effects in coccolith calcite. *Nat. Commun.* **8**, 14511 (2017).

5. Riebesell, U., Fabry, V. J., Hansson, L. & Gattuso, J.-P. *Guide To Best Practices For Ocean Acidification Research And Data Reporting* (Office for Official Publications of the European Communities, 2011).
6. Mills, G. A. & Urey, H. C. The kinetics of isotopic exchange between carbon dioxide, bicarbonate ion, carbonate ion and water. *J. Am. Chem. Soc.* **62**, 1019–1026 (1940).
7. Zhang, H., Torres-Romero, I., Anjewierden, P., Jaggi, M. & Stoll, H. *The DIC Carbon Isotope Evolutions During CO₂ Bubbling: Implications For Ocean Acidification Laboratory Culture*. <https://doi.org/10.31223/X5334W> (2022).
8. Keller, M. D., Selvin, R. C., Claus, W. & Guillard, R. R. Media for the culture of oceanic ultraphytoplankton 1, 2. *J. Phycol.* **23**, 633–638 (1987).
9. Zhang, J., Quay, P. D. & Wilbur, D. O. Carbon isotope fractionation during gas-water exchange and dissolution of CO₂. *Geochim. Cosmochim. Acta* **59**, 107–114 (1995).
10. Johnson, K. S. Carbon dioxide hydration and dehydration kinetics in seawater 1. *Limnol. Oceanogr.* **27**, 849–855 (1982).
11. Mehrbach, C., Culberson, C., Hawley, J. & Pytkowicz, R. Measurement of the apparent dissociation constants of carbonic acid in seawater at atmospheric pressure 1. *Limnol. Oceanogr.* **18**, 897–907 (1973).
12. Stoll, H. M. et al. Upregulation of phytoplankton carbon concentrating mechanisms during low CO₂ glacial periods and implications for the phytoplankton pCO₂ proxy. *Quat. Sci. Rev.* **208**, 1–20 (2019).
13. Rost, B., Zondervan, I. & Riebesell, U. Light-dependent carbon isotope fractionation in the coccolithophorid *Emiliana huxleyi*. *Limnol. Oceanogr.* **47**, 120–128 (2002).
14. Hermoso, M. Control of ambient pH on growth and stable isotopes in phytoplanktonic calcifying algae. *Paleoceanography* **30**, 1100–1112 (2015).
15. Phelps, S. R. et al. Carbon isotope fractionation in noelaerhabdaceae algae in culture and a critical evaluation of the alkenone paleobarometer. *Geochem. Geophys. Geosyst.* <https://doi.org/10.1029/2021gc009657> (2021).

Acknowledgements

This study was supported by the Swiss National Science Foundation (Award 200021_182070 to H.M.S.) and ETH Zurich core funding (ETH03-19-1 to H.M.S.).

Author contributions

H.Z. and H.M.S. designed the experiments. I.T.R. carried out the culture experiments with help of H.Z. H.Z. developed the numerical model. H.Z. and I.T. wrote the paper with input from H.M.S.

Competing interests

The authors declare no competing interests.

Additional information

Supplementary information The online version contains supplementary material available at <https://doi.org/10.1038/s41467-022-35109-4>.

Correspondence and requests for materials should be addressed to Hongrui Zhang or Ismael Torres-Romero.

Peer review information *Nature Communications* thanks the anonymous reviewer(s) for their contribution to the peer review of this work.

Reprints and permissions information is available at <http://www.nature.com/reprints>

Publisher's note Springer Nature remains neutral with regard to jurisdictional claims in published maps and institutional affiliations.

Open Access This article is licensed under a Creative Commons Attribution 4.0 International License, which permits use, sharing, adaptation, distribution and reproduction in any medium or format, as long as you give appropriate credit to the original author(s) and the source, provide a link to the Creative Commons license, and indicate if changes were made. The images or other third party material in this article are included in the article's Creative Commons license, unless indicated otherwise in a credit line to the material. If material is not included in the article's Creative Commons license and your intended use is not permitted by statutory regulation or exceeds the permitted use, you will need to obtain permission directly from the copyright holder. To view a copy of this license, visit <http://creativecommons.org/licenses/by/4.0/>.

© The Author(s) 2022